

Halved Vivaldi Antenna With Reconfigurable Band Rejection

Xavier Artiga, Julien Perruisseau-Carrier, *Member, IEEE*, Pablo Pardo-Carrera, Ignacio Llamas-Garro, *Senior Member, IEEE*, and Zabdiel Brito-Brito, *Member, IEEE*

Abstract—This letter presents a Vivaldi antenna having the capability of dynamically rejecting interferers, mainly aiming at multistandard communication with dynamic frequencies allocation. Only half of the Vivaldi is used and placed over a ground plane, which is suitable to vehicular communication. The rejection filter is integrated to the antenna real estate and consists of two microstrip resonators and two varactor diodes coupled to the slot of the Vivaldi. It is simply biased by applying the control voltage at the antenna RF port. Good matching is achieved from 2.5 to 8 GHz while rejecting a band whose central frequency can be tuned from 1.8 to 5.8 GHz. Simulated and measured return loss, gain, and radiation patterns are presented. The measured gain rejection in the direction of the radiation maximum is about 20 dB or better in the entire tuning range.

Index Terms—Antenna filtering, reconfigurable antenna, Vivaldi antenna.

I. INTRODUCTION

THE RECENT trend of integrating several functionalities and standards in a single device, as well as the efforts in software-defined and cognitive radio systems, has pushed the research on frequency reconfigurable antennas. It has been shown that tunable narrowband antennas exhibit good out-of-band rejection, thereby avoiding the need of (or relaxing the requirements on) the front-end filters [1]. However, such a solution becomes too complex as the number of independently controllable frequencies increases. On the other hand, a fixed multiband frequency antenna with a reconfigurable filter allows enabling or rejecting different frequencies, but does not allow the dynamic allocation of the frequencies. Finally, multiband antennas are not suitable in ultrawideband (UWB) systems. In this context, this letter addresses the implementation of a wideband antenna with a continuously tunable band rejection to simultaneously support different frequencies while dynamically rejecting interferers.

In [2] and [3], omnidirectional wideband antennas with embedded reconfigurable band rejections were presented. The

Manuscript received December 21, 2010; accepted January 18, 2011. Date of publication January 28, 2011; date of current version March 14, 2011.

X. Artiga, J. Perruisseau-Carrier, and I. Llamas-Garro are with the Centre Tecnològic de Telecomunicacions de Catalunya (CTTC), Barcelona 08860, Spain (e-mail: xavier.artiga@cttc.es).

P. Pardo-Carrera was with the Centre Tecnològic de Telecomunicacions de Catalunya (CTTC), Barcelona 08860, Spain. He is now with EADS-CAS-SIDIAN, Getafe 28906, Spain.

Z. Brito-Brito is with the Escuela Superior de Ingeniería Mecánica y Eléctrica (ESIME), Instituto Politécnico Nacional, D.F. 04430, Mexico.

Color versions of one or more of the figures in this letter are available online at <http://ieeexplore.ieee.org>.

Digital Object Identifier 10.1109/LAWP.2011.2108992

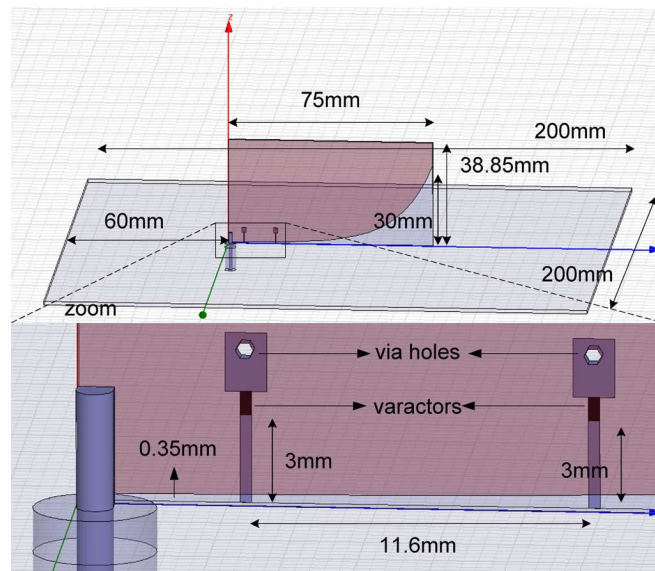


Fig. 1. Halved Vivaldi antenna.

antenna in [2] allows choosing between discrete rejection bands through the control of p-i-n diodes, whereas in [3], a MEMS switch is used to enable or disable a single fixed-frequency notch. In [4], several directive designs based on Vivaldi antennas are proposed, one of them concerning a reconfigurable band rejection. However, this design has not been actually implemented, and compared to this letter, it provides a much smaller simulated tuning range and would also require a dc biasing network.

In this letter, we present a Vivaldi antenna suitable for vehicle-to-vehicle communications, operating at 2.5–8 GHz with a stopband whose central frequency can be continuously tuned in the 1.8–5.8 GHz range. A halved Vivaldi over a ground plane is used for potential application in vehicular communication, but the same rejection scheme is directly applicable to standard complete Vivaldi antennas as used, e.g., in wideband phased arrays. In this case, embedding a reconfigurable filter in the Vivaldi slot would be useful if a differential LNA must be connected directly between the two disconnected Vivaldi “wings” [5].

II. ANTENNA DESIGN

A halved Vivaldi antenna placed perpendicular to a ground plane is used, as depicted in Fig. 1.

The idea is to take advantage of the presence of a vehicle metal surface in vehicular communications. If the antenna is located on a horizontal vehicle surface (e.g., roof), it would

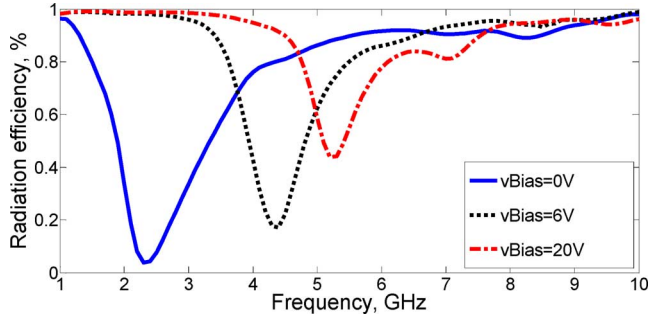


Fig. 2. Simulated radiation efficiency for three representative biasing voltages within the continuous tuning range.

present the radiation maximum at the horizon and a vertically polarized electric field. Moreover, as shown will be shown, the halved Vivaldi can be fed directly with a coaxial probe, avoiding the classical microstrip-to-slot-line transition.

From image theory, the fields radiated by the halved Vivaldi over an infinite ground plane are the same as using the complete antenna [6], whereas the antenna input impedance is half that of the complete Vivaldi. The halved antenna shown in Fig. 1 was optimized to be matched to a $50\text{-}\Omega$ reference impedance from 2.5 to 10 GHz.

The band rejection is achieved by a second-order bandstop filter directly integrated in the antenna real state for space considerations. It is formed by two microstrip line resonators placed across the slot in the antenna back plane. In fact, due to the presence of the ground plane, the resonators are also halved and must be soldered to the electrical symmetry plane constituted by the ground plane. The rejection band is then reconfigured by controlling the bias voltage of two varactors that connect the end of the microstrip lines to the ground plane (i.e., antenna plane) through via holes. Each varactor is essentially a capacitance (though in the modeling, a more accurate varactor circuit is used) terminating the microstrip lines, and therefore has a similar effect as adding a piece of line. Since the rejection frequency is determined by the effective length of the microstrip resonators, increasing the bias voltage—namely, reducing the varactors capacitance—results in an increased rejection frequency. It is noteworthy that placing the diode at the end of the resonators results in wider frequency tuning ranges for a given varactor model, which is the main reason for the large tuning range obtained here with regard to [4]. Moreover, the use of a second-order filter improves the notch selectivity and also allows the control of its bandwidth in the design stage.

It is noticeable that, in the proposed solution, no biasing network is required since the control voltage is directly applied between the coaxial central and ground conductors. The key feature of this solution (in contrast to most of the designs shown in [4]) is that strong currents excite the resonators and flow through the diodes only at the rejected frequencies. Therefore, as shown in Fig. 2, good radiation efficiency is preserved at desired frequencies while it decreases drastically at rejected frequencies, thereby improving the filtering performance. Moreover, the antenna radiation characteristics in the passband are not perturbed since the resonators are not excited.

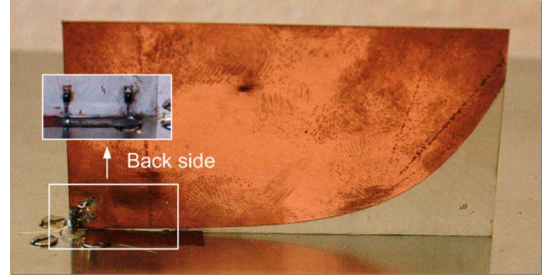


Fig. 3. Photographs of fabricated antenna.

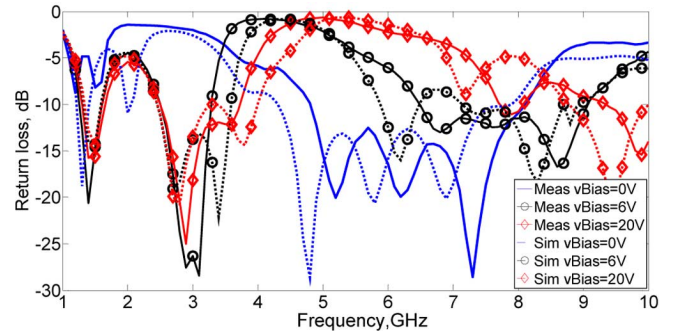


Fig. 4. Simulated and measured return loss for three representative biasing voltages within the continuous tuning range.

Finally it is worth mentioning that, if desired, more than one interferer could be rejected by cascading two filters or by designing a dual stopband filter

III. SIMULATION AND MEASUREMENT

The antenna was simulated using Ansoft HFSS and fabricated on a 0.5-mm-thick Arlon TC600 substrate of permittivity $\epsilon_r = 6.15$. The varactors chosen are MGV125-08-0805 from Aeroflex-Metelics. They are represented in the simulations by equivalent impedances previously extracted from TRL-calibrated diode measurements. The simulation was used for the fine optimization of the antenna and the embedded filter. A photograph of the fabricated antenna is shown in Fig. 3.

A. Return Loss

Fig. 4 depicts simulated and measured return loss for several diode biasing voltages. Wideband matching as well as wide stopband tuning range are achieved in both simulations and measurements. However, the measurements present a frequency shift and a widening of the rejection bands, which were shown to be attributable to moderate discrepancies between the real diode and the model included in the simulations. The fabricated antenna presents good matching from 2.5 to 8 GHz while rejecting a band whose central frequency can be tuned from 1.8 to 6 GHz, thereby covering the principle standards such as WiFi, WiMAX, Bluetooth, WLAN (802.11a), etc. The return loss is slightly degraded in the 3.75–4.8 GHz band due to this rejection band widening, but still remains better than 6 dB.

Although wideband rejection was targeted here, it was also shown that narrower rejection can be achieved by increasing

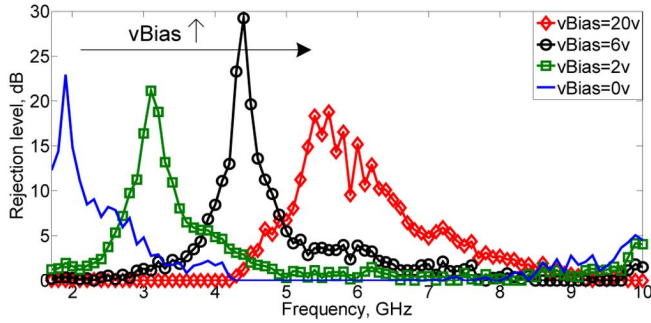


Fig. 5. Measured rejection level for four representative biasing voltages within the continuous tuning range.

and decreasing the diode equivalent inductance and capacitance, respectively (to keep the frequency unaltered). This can be achieved using two varactors in series. Another solution is to use other filter topologies such as microstrip u-shaped resonators placed close to the antenna slot.

B. Filtering Performance

For completeness, the antenna filtering performance is also evaluated in terms of the antenna gain in the direction of the radiation maximum. More precisely, this rejection level is defined as the difference between: 1) the maximum available gain within all bias voltages and 2) the gain of the antenna for the bias voltage under study. Therefore, this quantity represents the capability of the antenna to reject an interferer at a given frequency while communicating at other frequencies.

Fig. 5 shows the measured gain rejection for four representative bias voltages (only a limited number of states are shown here for clarity, but obviously a continuous tuning of the band rejection is achieved). We observe that a rejection between about 20 and 30 dB is achieved through the whole 1.8–5.8 GHz tuning range. Measured absolute gain values are 5 dBi at 2.5 GHz, 7.9 dBi at 5 GHz, and 11 dBi at 8 GHz (these values obviously correspond to the states where the antenna is matched at the measurement frequency).

C. Radiation Patterns

Finally, the antenna radiation patterns have been measured. To facilitate the fabrication and measurement process, the antenna has been placed over a limited-size aluminium plate, which thus cannot be considered as an infinite ground plane. Fig. 6 compares simulated radiation patterns for finite and infinite ground plane cases to the measured ones. Two frequencies (3 and 7 GHz), at which the antenna is well matched for a bias voltage of 6 V, are depicted. The directive property of Vivaldi antennas is verified, as well as a good agreement between simulations and measurements, except for the E-plane cross-polarized component. In measurements, this component

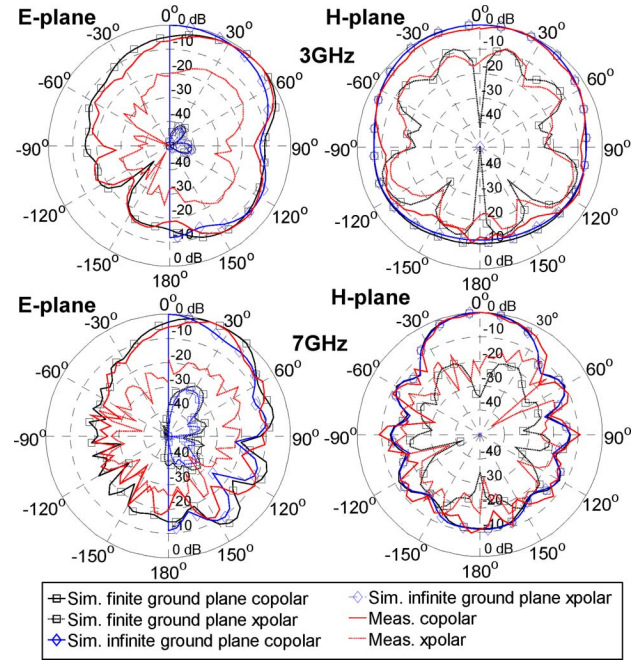


Fig. 6. Simulated and measured radiation patterns.

is 15 dB below the copolarized one and follows its shape, so we conclude that the discrepancies with the simulations are caused by the alignment precision in the measurement process. The principal effect of the finite ground plane is an elevation (45° at 3 GHz and 25° at 7 GHz) of the radiation maximum over the ground plane in the E-plane radiation pattern. The elevation angle is increased when the frequency is decreased since the ground plane becomes electrically smaller. Nevertheless, in most real applications, the ground plane would be large enough to behave as infinite, and this effect would not be relevant.

REFERENCES

- [1] S. Yang, C. Zhang, H. Pan, A. Fathy, and V. Nair, "Frequency-reconfigurable antennas for multiradio wireless platforms," *IEEE Microw. Mag.*, vol. 10, no. 1, pp. 66–83, Feb. 2009.
- [2] J. Perruisseau-Carrier, P. Pardo-Carrera, and P. Miskovsky, "Modeling, design and characterization of a very wideband slot antenna with reconfigurable band rejection," *IEEE Trans. Antennas Propag.*, vol. 58, no. 7, pp. 2218–2226, Jul. 2010.
- [3] S. Nikolaou, N. D. Kingsley, G. E. Ponchak, J. Papapolymerou, and M. M. Tentzeris, "UWB elliptical monopoles with a reconfigurable band notch using MEMS switches actuated without bias lines," *IEEE Trans. Antennas Propag.*, vol. 57, no. 8, pp. 2242–2251, Aug. 2009.
- [4] M. R. Hamid, P. Gardner, P. S. Hall, and F. Ghanem, "Review of reconfigurable Vivaldi antennas," in *Proc. IEEE APSURSI*, Jul. 11–17, 2010, pp. 1–4.
- [5] E. de Lera Acedo, E. E. Garcia, V. Gonzalez-Posadas, J. L. Vazquez-Roy, R. Maaskant, and D. Segovia, "Study and design of a differentially-fed tapered slot antenna array," *IEEE Trans. Antennas Propag.*, vol. 58, no. 1, pp. 68–78, Jan. 2010.
- [6] C. A. Balanis, *Antenna Theory: Analysis and Design*, 2nd ed. New York: Wiley, 1997.